

Chapter 2

Molecular Structure, Gating, and Regulation

Steen E. Pedersen

Abstract Gating of ion channels is the opening response of the channel to a stimulus and its subsequent desensitization or inactivation. For nicotinic acetylcholine receptors, the stimulus is the binding of the neurotransmitter acetylcholine to an extracellular domain followed by a sequence of conformational changes resulting in rapid channel opening. In most channels a persistent stimulus invokes a second gating event driving the channel into an inactive, desensitized state that may or may not contribute to the net response. A full understanding of gating requires a correlation of structural changes with the kinetics of channel opening and desensitization; an understanding of how these changes result in rapid, large changes in ion flux through the channel; and how they are terminated. In this article the current structural changes and the current understanding of nicotinic receptor channel kinetics are reviewed and correlated. The analysis necessarily draws on inferences from the larger family of ligand-gated ion channels and related proteins. The focus will be predominantly on the opening event but will also include consideration of desensitization.

Keywords Nicotinic acetylcholine receptor • Gating • Ligand binding • Conformational regulation • Linear free energy analysis • Allosteric ligand

Abbreviations

AChBP	Acetylcholine Binding Protein
ELIC	<i>Erwinia chrysanthemi</i> ligand-gated ion channel
GLIC	<i>Gloeobacter violaceus</i> ligand-gated ion channel
Glu-Cl	<i>C. elegans</i> glutamate-gated chloride channel
LFER	Linear free energy relationship
LGIC	Pentameric ligand-gated ion channel

S.E. Pedersen, Ph.D. (✉)

Department of Molecular Physiology and Biophysics, Baylor College of Medicine,
One Baylor Plaza, Houston, TX 77030, USA

e-mail: pedersen@bcm.edu

MWC	Monod-Wyman-Changeux cooperativity model
nAChR	Nicotinic acetylcholine receptor
TID	3-(trifluoromethyl)-3-(m-iodophenyl)diazirine
TM	Transmembrane domain

1 Introduction

The family of pentameric ligand-gated ion channels constitutes a class of fast synaptic neurotransmitter receptors (Fig. 2.1). This family includes the nicotinic receptors, the GABA_A receptors, the glycine receptors, and the 5-hydroxytryptamine receptors. The focus in this review will be on understanding gating of nicotinic acetylcholine receptors (nAChR), which are themselves divided into two classes: muscle-type and neuronal nAChR. The muscle-type receptors comprise 4 distinct subunits arranged pentamerically ($\alpha_2\beta\gamma\delta$ for the embryonic form; $\alpha_2\beta\epsilon\delta$ for the adult form). The neuronal forms comprise various mixtures subunit subtypes designated α_2 through α_{10} and β_2 to β_4 . The distribution and putative function of these receptors has been reviewed extensively [1] and will be addressed in detail elsewhere in this volume. Notably, subunits can mix as heteropentamers, e.g., $\alpha_4\beta_2\gamma_3$, or for some subunits, homo-pentamers, notably α_7 . However, structural and mechanistic information is derived from across the family; the receptors are all structurally similar, and, in broad strokes, likely undergo quite similar mechanisms of gating.

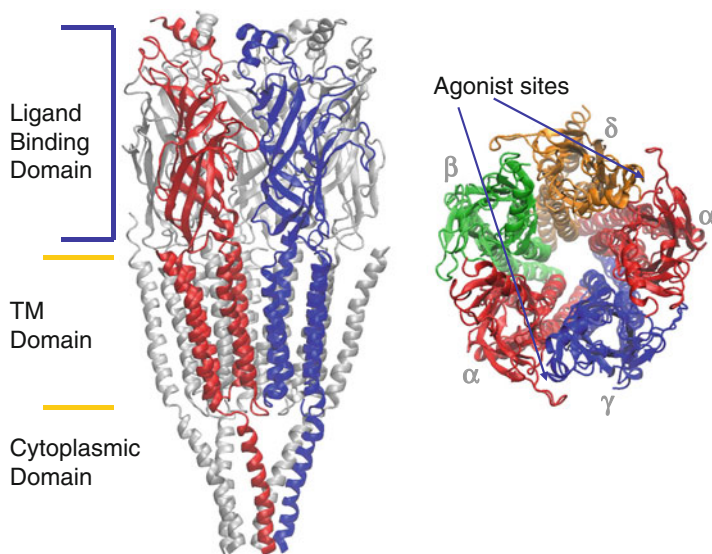


Fig. 2.1 Structure of the Torpedo nAChR. The *left* figure shows the *Torpedo* nAChR in cross-section. The *right* figure shows the receptor from the extracellular side [20]. The *arrows* indicate the location of the ligand-binding sites at the α - γ and α - δ subunit interfaces

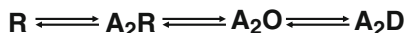


Fig. 2.2 A minimal model of nAChR activation. **R** represents the resting, or closed, conformation of the nAChR. **O** refers to the open, active conformation, and **D** the desensitized state. **A** refers to agonist or acetylcholine binding, occurring in two independent steps

The pentameric ligand-gated ion channels, as with most channels, have at least two gating actions: opening and desensitization. Both gating steps are ultimately initiated by the binding of neurotransmitter or ligand to binding sites. The binding first triggers rapid opening followed by desensitization; desensitization is entry into a nonconducting state that exists in the persistent presence of neurotransmitter. In practice, to analyze binding and single channel data, these are often described as chemical reaction steps in kinetic and thermodynamic schemes (see Fig. 2.2 for a simple example). Under ideal conditions, the opening step, or activation, can be isolated to a single elementary reaction, amenable to detailed kinetic and thermodynamic analysis. In contrast, desensitization, which is the equivalent of inactivation in voltage gated channels, appears to be a complex, multistep process, less amenable to a simple description; less is understood about this process.

High-resolution structural information on ligand-gated ion channels and some of their bacterial congeners has been forthcoming at an increasing rate and has shed a great deal of light on the possible mechanisms for opening and desensitization. These data are reviewed in the first section; for a more detailed review of structure-based analysis of the conformational changes, also see the excellent exposition by daCosta and Baenziger [2]. Nonetheless, a clear and comprehensive picture of gating at the level of the channel is still lacking. The second section considers the functional and indirect structural data that informs gating in the context of the high-resolution structural data.

2 Atomic-Resolution Structural Analysis of Gating

2.1 The Structural Basis of Gating at the Ligand-Binding Sites

As seen in Fig. 2.1, the family of pentameric ligand-gated ion channels constitutes pseudo-symmetric proteins with homologous or identical subunits surrounding a central pore that provides the ion conducting pathway. The ligand-binding event that triggers gating occurs in the extracellular (ligand-binding) domain. Structural studies on the homologous Acetylcholine Binding Protein (AChBP; [3–5]) and more recently on an $\alpha 7$ chimera [6] have provided a clear description of the structural changes that accompany binding within the ligand-binding domain.

As shown in Fig. 2.3 binding of agonists induces a pronounced change in the loop C region, an area of the protein that had already been identified as critical for ligand binding and characteristic of the α -subunits in the nicotinic receptor family. The idea that gating is triggered by a general inward movement of loop C was

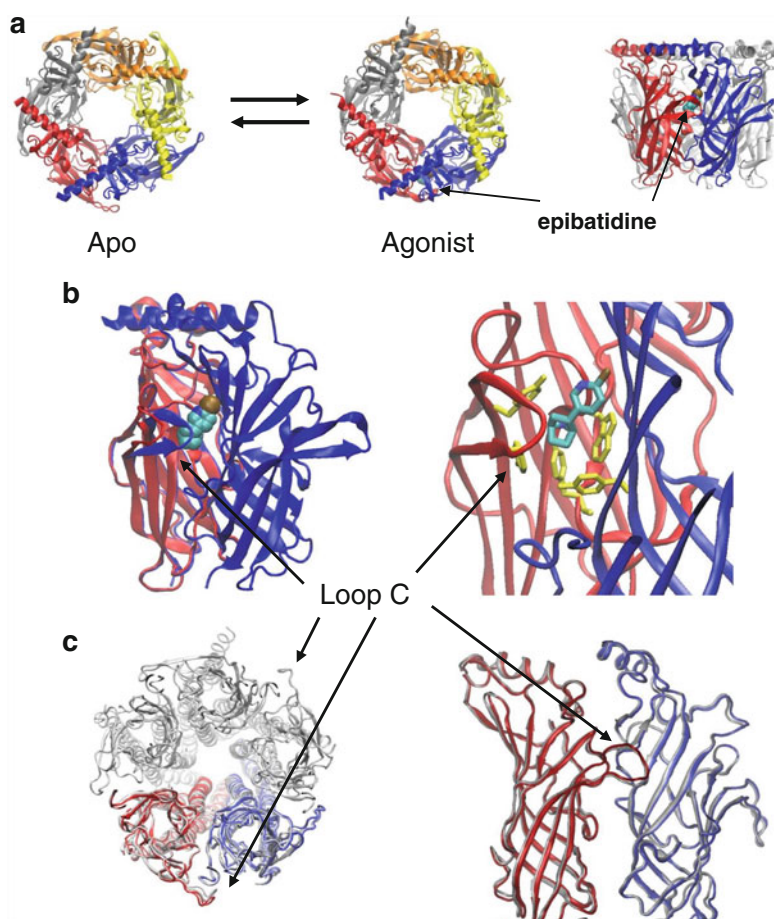


Fig. 2.3 Acetylcholine Binding Protein structures define agonist binding motions. Panel **a**, left, top views (extracellular side) of AChBP shown in its unliganded, apo form (pdb 2BYN) and bound to the agonist epibatidine (pdb 2BYP; [5]). Panel **a**, right, side view of the AChBP with epibatidine bound. Panel **b**, left, Superposition of individual subunit structures in the bound and unbound states: red—unbound; blue, bound. Panel **b**, right, detail of bound epibatidine surrounded by the aromatic residues known to stabilize cation binding. Panel **c**, Gating-changes in the nAChR Ligand-Binding Domain of the *Torpedo* nAChR by comparison of closed and open structures. Left side shows the open conformation in gray and the closed conformation colored for the α - and γ -subunits only. Panel **c**, right, shows details of the structural changes ascribed to opening

confirmed when antagonist binding was observed to interfere with loop closure [5]. This is consistent with the generally larger size of antagonists (e.g. conotoxin and *d*-tubocurarine) whereby a simple model of steric hindrance of loop closure prevents the normal loop C closure [5].

The details of further structural changes remain somewhat ambiguous. There are only modest changes in the overall β -sheet structure twist of the AChBPs between the two conformations (Fig. 2.3). The advantage of these high-resolution structures

as models for gating changes is mitigated by the absence of the conformational restrictions imposed by the presence of the transmembrane, channel domain and therefore, the relevant changes that communicate binding to the transmembrane domain may not be observed in AChBPs.

Data from full channels include recent electron microscopic structural investigations on the *Torpedo* nAChR. Changes in the extra-cellular domain seen by comparison of the electron-microscopic structures from Unwin's lab in the closed and open states also show only subtle changes (See Fig. 2.3c). The loops C are extended, similar to the unbound structure of the AChBP and the loop C changes upon opening are small relative to those seen in the AChBPs, but may give some indication of the general direction of those changes [7]. X-ray crystal data from the bacterial homologues ELIC [8] and GLIC [9], as well as several structures of the nematode Glu-Cl channel, which is also in the LGIC family [10] all show the loops C in a conformation similar to the agonist-bound AChBP structures. The structural data on loops C in the Glu-Cl channel is likely constrained by interaction with the cocrystallized FAB fragments [10]; whether gating in the bacterial channels involves changes in the extracellular domain is not known.

2.2 Binding Site Inequality

The two binding sites are nonequivalent. This is apparent from the structural organization of the heteropentamer in the muscle-type nAChRs (Fig. 2.1) in that elements from both the α -subunits contribute to binding, as well as elements of the adjoining subunits, the γ - and δ -subunits for the embryonic form of the muscle receptor. The site differences were first determined through *d*-tubocurarine binding and subsequent photoaffinity labeling studies with this compound identified the α - γ site and having higher affinity for *d*-tubocurarine and, through subsequent studies, lower affinity for agonist (acetylcholine and Dansyl-C6-Choline) in the resting state [11–13]. A number of chimeric and photoaffinity labeling studies identified residues responsible for the distinct agonist affinities in the γ -, δ -, and ϵ -subunits [14, 15], as well as for the antagonists *d*-tubocurarine, α -conotoxin, and α -bungarotoxin [16–19]. The affinity differences between the sites contribute substantially to shaping the dose-response curves in the embryonic $\alpha_2\beta\gamma\delta$ nAChRs; whereas in the adult $\alpha_2\beta\epsilon\delta$ form, the affinities are more or less equal. The studies identifying the sources of site-selectivity have been critical in identifying the key elements of the binding sites before atomic resolution structures became available. For obvious reasons, these differences do not apply to the homo-pentameric nAChRs, such as the α_7 nAChR. The consequences of site-selectivity will be discussed further under the functional aspects of gating.

A key question, not fully answered by the model studies on AChBP, is how the observed structural changes communicate the information to the transmembrane domain to affect opening of the pore. This question has been the topic of intense investigation through site-directed mutagenesis (see below).

2.3 The Structural Basis of Gating at the Channel

Substantial data have emerged showing a variety of LGICs with distinct structures in the channel region. High-resolution data from prokaryotic channels has shown clear, distinct structures from the two channels, ELIC [8] and GLIC [9]. These have been interpreted as reflecting closed and open states, respectively and the changes in the transmembrane region appear consistent with this interpretation (see Fig. 2.4). The nematode Glu-Cl channel also appears to be in an open conformation. However, two conformations, resting and open, determined on the same channel, the *Torpedo* nAChR, show only subtle differences and it is unclear whether those modest structural changes are sufficient to account for gating. But they may indicate the general shape and direction of the gating motion [7].

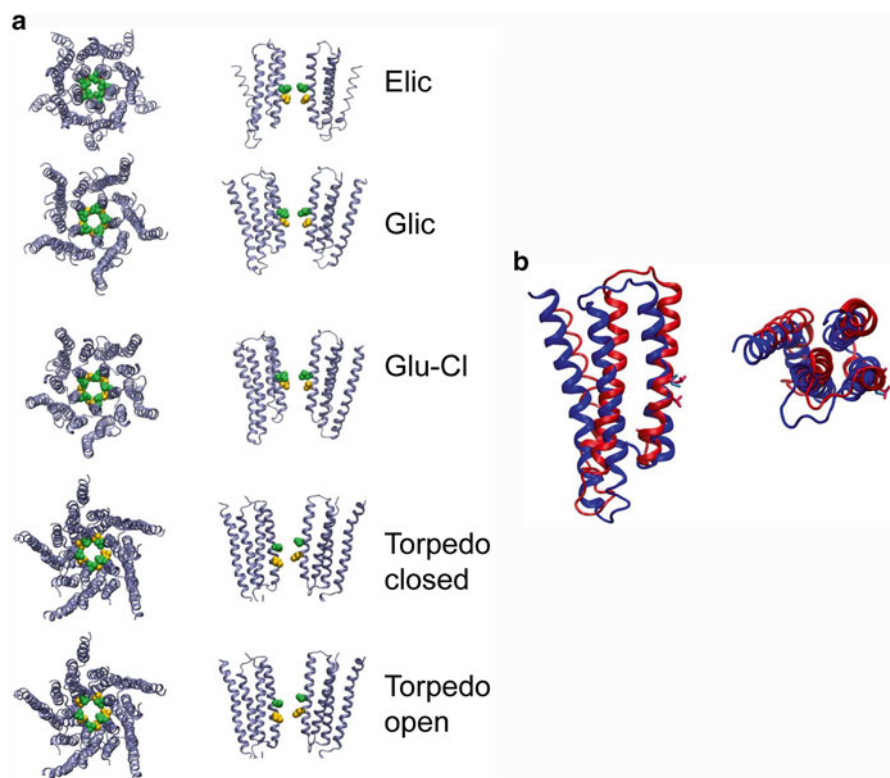


Fig. 2.4 Structures of the TM domain in open and closed conformations. Panel a, the left hand side shows the pentameric structure of the TM domain from the extracellular side. The right hand side shows the membrane cross section showing only two of the subunits, for clarity. Shown are: the ELIC channel (nominally closed, pdb 2VL0); the GLIC channel (pdb 3EHZ); the Glu-Cl channel, picrotoxin bound (nominally open, pdb 3RI5); *Torpedo* nAChR closed (pdb 4AQ5); *Torpedo* nAChR open (pdb 4AQ9). Panel b, side and top views of a single TM domain ELIC (red) and GLIC (blue) channels aligned. M1 was omitted in the side view for clarity

An initial EM structure of the *Torpedo* nAChR [20] showed a relatively accessible transmembrane (TM) domain that narrowed to a 6 Å diameter pore that was nonetheless apparently a closed structure (Fig. 2.1). The TM domain consists of four transmembrane α -helices from each subunit, named as M1 through M4. The M2-helices constitute the pore lining, and the M4-helix is the most exposed to the lipid milieu. This assessment was based on the apparent outward Loop C binding site configuration, indicating a conformation unbound by ligand and the general hydrophobicity of the pore (see Fig. 2.4). However the high-resolution structure of the prokaryotic channel ELIC revealed a few years later, showed a dramatically distinct TM-domain structure with much more closely apposed, straight and nearly parallel M2 α -helices [8]. This appeared more consistent with a generally closed structure where the close apposition of hydrophobic residues near the extracellular end of the channel clearly precludes ion permeation. Shortly thereafter, an acid-activated prokaryotic channel (GLIC) was crystallized, in low pH and the resultant structure indicated an apparent open-channel conformation [9, 21, 22]. The pore-lining M2 α -helices are splayed apart at the extracellular end and have sufficient space for ion permeation near the cytoplasmic end. The M2–M3 helices of ELIC and GLIC overlay nicely after an inward rotation of the helices from the splayed GLIC helices to those of ELIC. This suggests a simple outward and twist motion of the TM-helix bundle helices as a trigger for opening (see Fig. 2.4b).

This putative, open state was fairly consistent with the structures of the nematode Glu-C1 channel, that was crystallized in the presence of the endogenous agonist, glutamate, as well as in the presence of an open-channel blocker, picrotoxin, and in the presence of an allosteric activator [10]. These structures together argue for the Glu-C1 TM-domain being captured in an open state. Recent, higher-resolution structures of the GLIC channel reveal the presence of a hydrated sodium ion in what appears to be part of the selectivity filter of the channel. Further computer simulations on the ion pathway argue strongly for an open-channel configuration [23]. To further test whether the GLIC conformation reflected an open state, rather than an alternative closed state, cysteine crosslinks were engineered into GLIC. The cross-linked form demonstrated the capacity of GLIC to adopt a closed-like conformation, similar in structure to that of ELIC, as determined by crystallography [24], and shown to be nonconducting.

The apparent contradiction between these structures and the quite subtle changes found for the *Torpedo* nAChR are not readily reconciled. The *Torpedo* structure shows quite modest changes upon agonist exposure, both at the agonist sites and the level of the TM domain [7]. The TM domain in the putative closed state is closer to the open configuration as defined by the GLIC and Glu-C1 structures. However, the ligand-binding domain appears to be in an unliganded conformation. Given the close coupling between binding and opening and desensitization, it is unclear whether the gating movement in the *Torpedo* nAChR is fundamentally subtler or whether the inability to determine the absolute conformation in crystal structures simply confounds interpretation.

2.4 Structural Basis of Coupling Ligand Binding to Channel Gating

The ligand-binding and transmembrane domains are distinct structures, the former being predominantly β -sheet and the latter largely α -helical. The interface is where communication between the ligand-binding event and the channel must take place. The primary features of the interface thought to mediate this are loops intertwining from the ligand-binding domain and the TM domain. The Cys-loop ($\beta 6$ – $\beta 7$ loop), which contains the disulfide bond conserved among the eukaryotic LGIC subunits, and the $\beta 1$ – $\beta 2$ loop (See Fig. 2.5) surround the M2–M3 linker on the TM domain (the loop linking the M2 and M3 TM α -helices). Mutational analysis early on identified the M2–M3 linker as a critical aspect of communication between the extracellular domain and the TM domain [25, 26]. In addition, there is a direct connection between the $\beta 9$ – $\beta 10$ sheet (which includes the Loop C structure that binds agonist), and the first transmembrane domain, that seems likely to exist for communication between ligand-binding and the TM-domain. The motions triggered by ligand binding likely communicate these changes to the TM domain through movements in these linkers. There is substantial mutational evidence (see below) for communication between these loops, but the conclusions from the structures is less enlightening about motions that could effect the large changes seen among the putative closed and open channel structures.

Comparison of putative open (GLIC and Glu-Cl) or closed (ELIC) structures do not show obvious changes in this region that lead to a clear hypothesis of communication. The M2–M3 linker is longer for these channels than in the *Torpedo* nAChR. The recent comparative structures of the *Torpedo* nAChR channel show very small changes in the motion of the linkers, as well as only small motions in the rest of the protein, upon agonist binding. The smaller linker in the nAChR primarily engages the Cys-loop ($\beta 6$ – $\beta 7$ loop) and the $\beta 1$ – $\beta 2$ loop, which surround the highly conserved proline residue whereas in the prokaryotic channels and in Glu-Cl the M2–M3 linker has one helix coil unwound and interacts with the adjacent subunit as well (Fig. 2.5).

In summary, it seems apparent and logical that tension generated by ligand binding likely affects the $\beta 9$ – $\beta 10$ loop, which connects directly to the TM domain at M1,

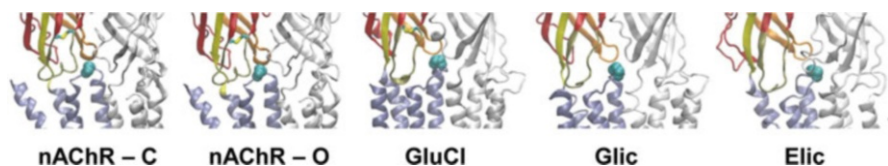


Fig. 2.5 Structures of the Domain interface and the coupling region. The M2–M3 linker is shown with the conserved proline in van der Waals dimensions. The $\beta 10$ sheet is shown in yellow, the Cys-loop in tan, and the $\beta 1$ – $\beta 2$ loop in orange. The pdb accession codes for the structures are nAChR closed (nAChR-C), 4AQ5; nAChR open (nAChR-O), 4AQ9; Glu-Cl, 3RI5; GLIC, 3EHZ; ELIC, 2VLO

and likely involves motions of the Cys-loop ($\beta 6$ – $\beta 7$ loop) and the $\beta 1$ – $\beta 2$ loop acting on the M2–M3 linker. While it is clear from the structural analysis and from mutational analysis that these regions are critical for communication between the extracellular domain and the transmembrane domain, nonetheless, a clear description of how ligand binding alters the conformation in this region and communicates the movement to the channel, is still lacking. This is partly because the prokaryotic channels do not evince the same extracellular ligand binding as the eukaryotic channels, possibly due to crystal constraints, and to the modest structural changes seen in the careful comparisons of the closed and activated *Torpedo* nAChR [7].

2.5 Desensitization

An added layer of complexity in our understanding of the structural basis of gating is introduced when we consider desensitization for LGICs [27]. The *Torpedo* nAChR is well-known to desensitize readily under the influence of a number of local anesthetics, detergents, and other agents, as well as in the prolonged presence of conventional agonists such as acetylcholine [28–32]. However, ambiguities in the functional state of channels where we have high-resolution structures make it unclear whether any of those structures fully define a distinct functional state. Is it possible that the ELIC structure or the nAChR structure represents a desensitized state rather than a simple closed configuration? This appears unlikely considering several general observations. Photo-affinity labeling studies have identified residues that change their exposure, or reactivity, or both when changing from closed to open to desensitized; channel blockers that preferentially bind the resting state, such as tetracaine [33] and 3-(trifluoromethyl)-3-(m-iodophenyl)diazirine (TID) are typically smaller, while the desensitized channel can accommodate substantially larger ligands such as meproadifen mustard, ethidium, and crystal violet. Large channel blockers display slow kinetics of binding and egress from the desensitized channel, indicating restricted access in the desensitized state [32, 34]. Yet, structural features consistent with restriction of ligand access to the channel pore have not been observed in any of the crystal structures, so it is possible that none of the known structures are representative of the desensitized state.

2.6 Summary of Structural Data

High-resolution structural data have provided a wealth of information on the basic structure of the channel. It provides a clear picture of changes in the ligand-binding domain, and also about possible changes that may constitute gating within the TM domain. The actual location of such conceptual features as the gate, the element that restricts flow in the closed state, and the selectivity filter, are less clear, given the distinctions between the nAChR structures and the bacterial LGICs. Other types of

indirect structural information, such as accessibility studies and photo-affinity labeling, along with functional analysis further informs the structure and location of these features as discussed below.

3 Functional Analysis of Gating

Gating of nAChRs has been analyzed extensively using electrophysiology, ion flux assays, ligand-binding assays, and single channel recordings. These have been combined with such techniques as photoaffinity labeling and cysteine accessibility assays to probe the structures and structural changes at various sites on the receptor. These techniques have their distinct advantages and taken collectively present a reasonably cohesive, though incomplete, picture of gating in nicotinic receptors. The combination of single amino acid substitution, single channel gating measurements, and thermodynamically-based analysis is proving a powerful technique that provides substantial functional information on the role of individual amino acids in gating. It also provides insight into the order of events during the gating transition.

nAChR activation typically requires high micromolar concentrations of acetylcholine, which are substantially higher than the low nanomolar concentrations determined to bind fully at equilibrium [28, 35, 36]. nAChRs were closed at conditions of equilibrium binding, thereby describing the nonconducting desensitized state as having high affinity for acetylcholine [27]. These observations essentially set the stage for the current model of nAChR-activation and desensitization (see Fig. 2.2). Although a number of details embellish this model, as discussed below, this model captures the main, essential features of nAChR activation as we currently understand it.

One goal of functional studies is to determine the number of stable and intermediate states of the nAChRs so as to arrive at a complete energetic and structural description. The atomic-resolution structural information lags behind due to the inherent difficulty of crystallization. Therefore, functional studies are critical to understanding the basic route that activation and desensitization can occur and thereby inform basic structural constraints. The current questions include whether there are intermediate states between ligand binding and channel opening and between opening and full desensitization.

3.1 *Energetics and Linear Free Energy Analysis of Gating*

The energetics of gating can be examined through the effect of mutational changes on the overall gating equilibrium between the closed and open states (Figs. 2.2 and 2.6). This informs the amino acids that are critical in the gating motion or can affect it allosterically. A refinement of this analysis that provides a distinct element of information is Linear Free Energy Analysis (LFER; or Φ -value analysis). This requires an assumption that the closed-to-open state transition can be described as

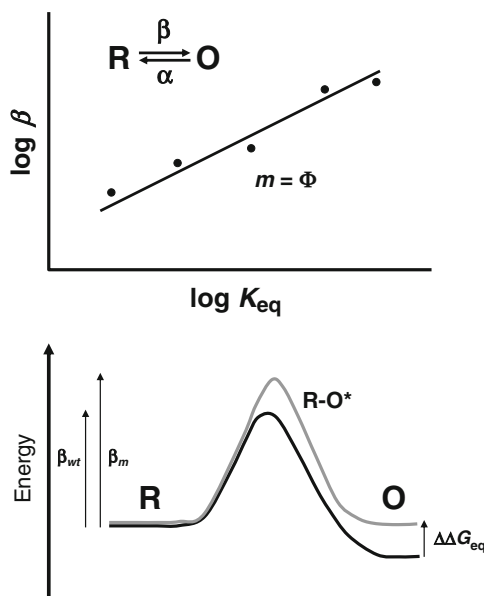


Fig. 2.6 Linear Free Energy Analysis. *Top*, the gating transition is confined to being described as a simple elementary reaction between **R** and **O** states with rate constants β (forward) and α (backward). The ratio β/α describes the equilibrium constant, K_{eq} . A plot of $\log \beta$ versus $\log K_{eq}$ from mutations or other perturbations at a discrete site is described by the slope Φ , which is a descriptor of how close the transition state (**R-O***) is to the open state structure, ranging from zero to one. *Bottom*, a schematic of the transition state diagram for *wt* and mutant (*m*) nAChR between the open and closed states. The diagrams for the two nAChRs are arbitrarily aligned at the resting state energy, showing changes in the equilibrium constant free energies ($\Delta\Delta G_{eq}$). The *arrows* at the left correspond to the activation energies associated with the forward rate constants β and are proportional to $\log \beta$

an elementary chemical transition and examines the gating transition state at any amino acid where a mutation perturbs gating. Based on perturbation of the closed-to-open equilibrium, the principles of the analysis are derived from basic thermodynamics and reaction kinetics. Grosman et al. [37] described its application to the nAChR: the technique requires single channel analysis of opening and closing rates (β and α , respectively). These also determine the overall equilibrium between the two states (see Fig. 2.6). Upon perturbation of the equilibrium through mutation or using various agonists, a log plot of β *versus* the equilibrium constant provides a slope, a Φ -value. The higher the slope for the forward rate constant the greater the transition state resembles the open state. This interpretation reflects the lack of change in the rate constant from open to closed, suggesting little perturbation between the open state and the transition state (Fig. 2.6b). For plots of the closing constant, α , the reverse argument holds true, high slopes reflect low Φ values and reflect a transition state that more closely approximates the closed state. By carrying out Φ -value analysis on the binding site and on other amino acids thought to be

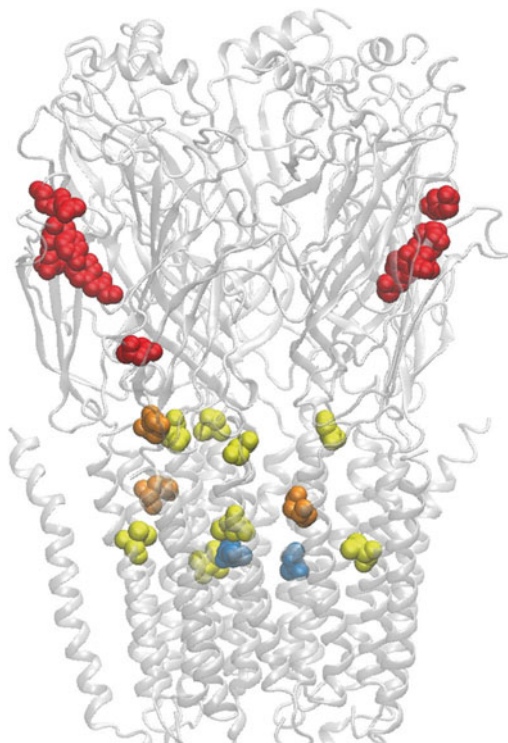


Fig. 2.7 A structural illustration of Φ -value analysis. The structure illustrates a few amino acids from the various zones of high, intermediate and low Φ -values. The residues are colored according to Φ -value ranges with the data taken from Grosman and Auerbach [37]: *Red* indicates a range of 0.9–1; *yellow*, 0.7–0.9; *orange*, 0.4–0.7; *blue*, 0–0.4. Subsequent work has fleshed out these results to show there are four distinct regions of similar Φ -values. These are not restricted to distinct domains but have some structural overlap. In general, amino acids closer to the binding site have higher Φ -values and those at the gating region and channel, lower Φ -values. Higher values indicate that the transition state structure is more like the open state; lower values more like the closed state. The four regions may indicate parts of the structure that move coordinately during the transition from closed to open

involved in gating, Auerbach and colleagues mapped the transition state patterns of the gating movement throughout the mouse muscle nAChR [38].

The results of this analysis reveals a pattern where the binding site more closely resembles the open state and parts of the channel more closely resemble the closed state during the transition state [39] (see Fig. 2.7 for a limited sample of residues tested). This appears to make sense as ligand-binding drives channel opening through an induced-fit mechanism [40] that is energetically driven by cation– π interactions between acetylcholine and the aromatic side chains of the binding site [41–43]. The binding provides the ultimate strain that drives opening, so it is expected that this should more closely resemble the final, high-affinity open state. Likewise, it is not unexpected that the channel and the physical gate would more

closely approximate the closed state. The full data set paints more detail on this simple picture of strain communicated from the binding site to the gate.

The Φ -values reflect the overall change of the transition state relative to the starting and end states. Thus, amino acids with similar Φ -values like move in a tightly-coupled manner. That is, by identifying the regions where the Φ -values changes, there will be greater flexibility in transmission of the strain from the binding site to the gates. This can give insight into the motions of the nAChR as it undergoes channel opening. Using this approach Auerbach's group [38] identified several areas that move in relative synchrony. These begin with a cluster in the ligand-binding site where Φ -values are close to one. Lower values occur in the other parts of the ligand-binding domain, including the region where linkage to the transmembrane domain occurs, and in the transmembrane domain. By identifying four distinct regions with similar Φ -values, the data argue for regions moving in blocks during the transition.

3.2 *Where Is the Actual Gate?*

Gating was initially proposed to lie near the conserved 9'-Leu that appeared congruent with a bend in the M2 helix [44, 45]. Consistent with this hypothesis is the profound effect of mutagenesis of this residue on the gating equilibrium [20, 44, 46, 47]. The structural studies on the nAChR are generally consistent with Substituted Cysteine Accessibility Measurements (SCAM) from Karlin's group, which showed the closed and open states to have a number of residues in M2 accessible in both states, but with residues deeper in the channel, near the intracellular end of M2, being accessible only in the open state [48]. This identified the cytoplasmic region of M2 as the effective gating structure. Modeling indicates that even with a relatively large-diameter pore in the closed state, change in hydrophobicity can affect conductivity dramatically. Thus, gating can be described as a local change in hydrophobicity due to modest changes in pore size and side-chain exposure. This can affect the ability a partly hydrated ion to permeate the pore [49]. This hydrophobicity change is likely accomplished either by twisting the M2 helices such as to change the exposure from hydrophobic to hydrophilic residues, or, as has been argued by Cymes et al. based on proton modification, a modest increase in the diameter at this region [50]. However, the model of gating evinced by the differences between ELIC and GLIC structures shows more dramatic changes, and gating may reflect larger overall changes in structure (see Fig. 2.4).

3.3 *The Flip Side of Activation*

Colquhoun's group initially proposed the existence of an intermediate state of activation based on experiments on the glycine receptor [51, 52]. This scheme is illustrated in Fig. 2.8 (for nAChRs) and shows a proposed state required to account for

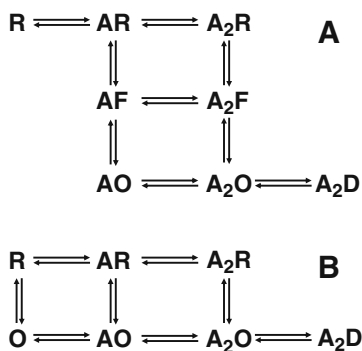


Fig. 2.8 Models for nAChR activation. Panel **a**, the model includes a pre-open, global flip state, with intermediate affinities for agonist. This state is hypothesized to be an intermediate transient state from which opening occurs. There is no direct transition from the initial, low-affinity binding state, **R**, to the open state, **O**. Based on the description by Lape et al.[53], the **F** (flip) state is include in models to adequately account for brief closing events in the presence of partial agonists. Panel **b**, a classic MWC-type model for opening [43, 77]

data from single channel measurements of short closing times, which are not accounted for by simpler models, but that also occur in the same time domain as open-channel block. It was further argued that this mechanism applies also to the nAChR on the basis of experiments using the partial agonists choline and tetramethyl ammonium [52, 53] on human muscle nAChR. The addition of this intermediate affinity, flip state (see Fig. 2.8), closed conformation may explain these observations, although it has been argued that it is unnecessary to account for agonist gating in the mouse muscle-type nicotinic receptor [43, 54] and that a typical MWC model accounts adequately for activation (Fig. 2.8b). Nevertheless, the addition of a new state to the repertoire of intermediate and quasi-stable states may require further structural characterization for a complete understanding of the movements of the LGICs as they activate.

3.4 Desensitization as a Gating Phenomenon

Desensitization is characterized by high agonist affinity and by a nonconducting channel and occurs spontaneously upon prolonged exposure to agonist or tetanic stimulation of a muscle endplate [27]. In the muscle-type nAChR, desensitization occurs relatively slowly, typically taking greater than 50 ms [28, 29, 35, 55]. This makes it unlikely to have a physiological role during typical moderate endplate stimulation but may be important during tetany or under pathological conditions. Some neuronal nAChRs desensitize substantially faster, particularly the $\alpha 7$ homo-pentameric subtype. In those cases it is likely that desensitization plays a role in

terminating the response to acetylcholine [56, 57]. Desensitization is less-well understood relative to our understanding of opening, despite its initial thorough characterization on the *Torpedo* nAChR [28, 29]. This partly reflects the difficulty of characterizing a nonconducting state that exits from the open state (Figs. 2.1 and 2.8b). Surprisingly, as it is the mostly stable bound state, it is yet unclear if any of the structures discussed above reflect a desensitized state rather than a closed state.

As noted by Katz and Thesleff [27], the desensitized state is the thermodynamically most stable state and should reflect the highest agonist-affinity. However, thermodynamic cycle analysis and measurements of ligand binding and open probabilities show that the open state also has high affinities for acetylcholine [58] that do not appear to differ appreciably from measured affinities of acetylcholine for the desensitized state [59].

This is a critical observation because it indicates that there is likely little, if any change in the ligand-binding affinity, and perhaps, little to no change in structure of the ligand-binding domain (acetylcholine cannot induce a structural change to a conformation with similar or lower affinity). Thus, structural changes in the progression from the open to desensitized state may be confined to the transmembrane domain. How can the desensitized state be more stable and have the same agonist affinity as the open state? This can be true if the unliganded desensitized state is also more stable than the open state. And this is generally true—the unliganded open state is quite rare (10^{-6} or so). But the unliganded resting-desensitized equilibrium is more modest (0.05 in *Torpedo*; a bit lower in mouse muscle). That implies a strong, residual unliganded open to desensitized equilibrium ($\sim 10^4$; see also Fig. 2.9), which will be similar for the open to desensitized transition. This conclusion has important implications for any drug-discovery efforts that hope to differentiate between activation and desensitization of the nAChR, as might be useful for treatment of nicotine addiction. Drugs targeted to the agonist sites that activate may inevitably lead to desensitization and reinforce any addiction mediated by desensitization. Therefore allosteric activators may be better choices for such future therapeutics.

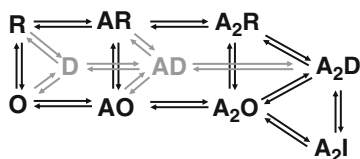


Fig. 2.9 MWC Model for desensitization. The schematic shows several possible routes for desensitization. The predominant route is undoubtedly through doubly-liganded binding to opening to the desensitized state. Some nAChRs, such as the *Torpedo* muscle type, have a substantial population in the preexisting desensitized state (in gray), which bind agonist with intrinsically high affinity. Desensitization from the open state like proceeds through one or more intermediate, structurally distinct states (I)

Desensitization involves rendering the channel nonconductive. In principle, it is possible that the channel reverts to the resting, or closed, state, while the ligand-binding domain remains in a high-affinity conformation, effectively uncoupling binding from channel gating. However, a substantial body of evidence indicates that the channel occupies a structurally distinct state when desensitized. This evidence comes from photoaffinity labeling studies, from cysteine accessibility studies, and from kinetic studies of ligand binding by channel blockers.

Photoaffinity labeling of the nAChR, using compounds such as Chlorpromazine and [125 I]TID, show clear changes in labeling patterns in the various states, including closed, open, and desensitized [60–65]. A large number of ligand-binding studies on various channel blockers, including local anesthetics and detergents, show substantial changes in affinity upon desensitization [31, 66, 67]. This clearly demonstrates a change in affinity for channel blockers between the closed state and the desensitized state. Conversely, binding of these ligands also cause changes in the affinity of agonists: desensitizing ligands, such as ethidium, effectively increase the equilibrium affinity of agonists; channel blockers such as tetracaine, which preferentially bind the closed state, lower the effective acetylcholine affinity [30, 33].

Binding kinetics may provide further insight into the structure of the desensitized state. In one example, the binding affinity of the fluorescent channel blocker ethidium is increased by agonists, and decreased by α -bungarotoxin, which stabilizes the closed state [67, 68]. It binds rapidly to the open channel upon brief exposure to agonist, dramatically increasing the effective association rate [69]. However, once desensitized the dissociation rate for ethidium is slowed dramatically [67, 70]. This indicates that egress of the ligand from the channel is structurally impeded. The ethidium site has also been identified through photo-affinity labeling and binds at the mid- level (near 12') of the M2-alpha helix [12, 71]. Notably, the current structures of the nAChR appear relatively open at the level of the binding site. So the kinetic data argues for a novel, as yet uncharacterized conformation with the channel impeded above the level of the ethidium site. Data from photoaffinity labeling with chlorpromazine in well-defined functional states further demonstrate structural changes in this region between the closed and desensitized states [63].

3.5 *The Intermediate State of Desensitization*

Desensitization has been characterized typically as “fast” and “slow” or alternatively “intermediate” and “full”, reflecting the distinction between functional desensitization and the somewhat slower acquisition of slowly-reversible, high affinity agonist binding [28, 35]. Initial electrophysiological characterization of desensitization shows it taking place with multiple time constants [55, 72]. A detailed electrophysiological study of the kinetic constants of desensitization on the mouse muscle receptor showed up to five distinct time constants associated with desensitization [73].

Time-resolved photoaffinity labeling by a small hydrophobic 3-(trifluoromethyl)-3-(*m*-iodophenyl)diazirine (TID) further elucidated distinct structural changes at the level of the middle of M2 upon fast desensitization and near the cytoplasmic end upon slow desensitization (see Fig. 2.9). These indicated changes associated with fast and slow desensitization that were distinct within the channel domain and clearly distinct from the labeling patterns of the resting (closed) channel [74, 75]. Unlike intermediate closed states, the existence of intermediate desensitized states is clear. Early data based on the binding of fluorescent analogs of acetylcholine showed several exponential phases of binding [76]. Though these seemed to correlate with intermediate affinities of acetylcholine binding prior to full long-term desensitization the changes do not actually necessitate a change in agonist affinity, but likely reflect changes in the transmembrane domain alone. Both of these assays establish intermediate states before acquiring the slowly reversible high affinity for acetylcholine that is the hallmark of the fully desensitized state. A Monod-Wyman-Changeux (MWC) [77]-type model for these states is shown in Fig. 2.9.

3.6 The Role of Multiple Binding Sites

The heteropentameric structure of the embryonic muscle-type receptor ($\alpha_2\beta\gamma\delta$) results in highly distinct affinities for agonist at the two sites, which subsequently affects the dose-response curve of these proteins. The affinities for the agonists differ ~ 100 fold in the resting state, but only \sim threefold in the desensitized state [13]. For the *Torpedo* nAChR, the α - δ site has higher affinity for agonist in both states. In the resting state the α - δ site affinity is about $1\ \mu\text{M}$, as compared with $\sim 100\ \mu\text{M}$ for the α - γ site [13]. Since channel opening is dominated by biliganded opening events the dose response curve follows binding to the α - γ site, to a first approximation, as the α - δ site will be occupied at much lower concentrations. Because the affinities of the sites are closer in the desensitized state, the α - γ site undergoes a larger change in affinity upon conformational changes to the open and desensitized states. Therefore, most of the energy driving the conformational change is provided through the α - γ site [13, 78]. For the mouse muscle adult form of the nAChR, $\alpha_2\beta\epsilon\delta$, the two affinities are nearly equal and the two sites contribute to the dose-response curve and the energetics more equally.

An interesting question arises for the homomeric receptors, such as α_7 , as to how many of the potentially five equivalent sites are required for activation. Work by Rayes et al. [79], in α_7 -5HT_{3A} chimeric receptors suggests that two nonconsecutive sites are sufficient for effective activation (i.e. sites with an intervening subunit). Three sites are most efficacious, and this provides the rationale for the efficacy of allosteric activators such as benzodiazepines in GABA_A receptors *via* binding to a third, nonconsensus site, that does not normally bind agonist [80]. Interestingly, this work found the same locus to be most efficacious and this site is equivalent to the δ - β interface on the muscle-type receptor (Fig. 2.1). It also suggests which interface may be a good target for allosteric therapeutic ligands.

4 Summary, Conclusions, and Unresolved Issues

The prevailing questions for understanding gating of the nAChRs are now focused on a detailed correlation between structure and function. Atomic resolution structures have provided a clear picture of gating at the level of the ligand-binding sites. This information is being brought to bear in drug development, particularly for treatment of disorders of the central nervous system [1]. In contrast, there are major outstanding questions as to whether the bacterial protein structures or those from the *Torpedo* nAChR better represent the gating transition that need to be resolved.

Although not unique to these channels nor to channels in general, it should be noted that proper ligand-gated channel function is highly dependent on the detailed kinetics of the mechanism. As one example, one instance of congenital myasthenia gravis turned out to be a mutation that had a modest two-fold effect on the channel gating efficiency [81]. In many proteins and enzyme such an effect on would have little to no impact on its functionality. In this respect, ion channels present an excellent model system for understanding conformational regulation and kinetic control of proteins at a detailed level. Functional studies, through the use of single-channel current measurements, presents great opportunities for detailed kinetic studies. Combined with single amino acid substitution they constitute a rich methodology for probing the roles of individual residues in function. Ultimately, the detailed structural knowledge must be correlated closely with these kinetic models to provide an overall understanding of these functions.

In summary, understanding and correlating the structure and function of ligand-gated ion channels presents a unique opportunity to probe deeply our understanding of the kinetic control of proteins in general. In addition, such detailed knowledge will provide additional information for the development of specific therapeutics targeting ligand-gated ion channels. The worth of allosteric ligands [1] has been proven in the GABA receptors, and therefore the nicotinic receptors provide a rich new area for similar types of intervention to help treat a number of disorders, the most prominent of which may be cigarette addiction.

Acknowledgements All molecular modeling figures were created using VMD [82].

References

1. Taly A, Corringer PJ, Guedin D, Lestage P, Changeux JP. Nicotinic receptors: allosteric transitions and therapeutic targets in the nervous system. *Nat Rev Drug Discov*. 2009;8(9):733–50.
2. Dacosta CJ, Baenziger JE. Gating of pentameric ligand-gated ion channels: structural insights and ambiguities. *Structure*. 2013;21(8):1271–83.
3. Smit AB, Syed NI, Schaap D, van Minnen J, Klumperman J, Kits KS, Lodder H, van der Schors RC, van Elk R, Sorgedrager B, Brejc K, Sixma TK, Geraerts WP. A glia-derived acetylcholine-binding protein that modulates synaptic transmission. *Nature*. 2001;411(6835):261–8.

4. Brejc K, van Dijk WJ, Klaassen RV, Schuurmans M, van Der Oost J, Smit AB, Sixma TK. Crystal structure of an ACh-binding protein reveals the ligand-binding domain of nicotinic receptors. *Nature*. 2001;411(6835):269–76.
5. Hansen SB, Sulzenbacher G, Huxford T, Marchot P, Taylor P, Bourne Y. Structures of *Aplysia* AChBP complexes with nicotinic agonists and antagonists reveal distinctive binding interfaces and conformations. *EMBO J*. 2005;24(20):3635–46.
6. Li SX, Huang S, Bren N, Noridomi K, Dellisanti CD, Sine SM, Chen L. Ligand-binding domain of an α 7-nicotinic receptor chimera and its complex with agonist. *Nat Neurosci*. 2011;14(10):1253–9.
7. Unwin N, Fujiyoshi Y. Gating movement of acetylcholine receptor caught by plunge-freezing. *J Mol Biol*. 2012;422(5):617–34.
8. Hilf RJ, Dutzler R. X-ray structure of a prokaryotic pentameric ligand-gated ion channel. *Nature*. 2008;452(7185):375–9.
9. Hilf RJ, Dutzler R. Structure of a potentially open state of a proton-activated pentameric ligand-gated ion channel. *Nature*. 2009;457(7225):115–8.
10. Hibbs RE, Gouaux E. Principles of activation and permeation in an anion-selective Cys-loop receptor. *Nature*. 2011;474(7349):54–60.
11. Neubig RR, Cohen JB. Equilibrium binding of [3H]tubocurarine and [3H]acetylcholine by Torpedo postsynaptic membranes: stoichiometry and ligand interactions. *Biochemistry*. 1979;18(24):5464–75.
12. Pedersen SE. Site-selective photoaffinity labeling of the Torpedo californica nicotinic acetylcholine receptor by azide derivatives of ethidium bromide. *Mol Pharmacol*. 1995;47(1):1–9.
13. Andreeva IE, Nirthanan S, Cohen JB, Pedersen SE. Site specificity of agonist-induced opening and desensitization of the torpedo californica nicotinic acetylcholine receptor. *Biochemistry*. 2006;45(1):195–204.
14. Prince RJ, Sine SM. Molecular dissection of subunit interfaces in the acetylcholine receptor. Identification of residues that determine agonist selectivity. *J Biol Chem*. 1996;271(42):25770–7.
15. Pennington RA, Gao F, Sine SM, Prince RJ. Structural basis for epibatidine selectivity at desensitized nicotinic receptors. *Mol Pharmacol*. 2005;67(1):123–31.
16. Chiara DC, Xie Y, Cohen JB. Structure of the agonist-binding sites of the Torpedo nicotinic acetylcholine receptor: affinity-labeling and mutational analyses identify gamma Tyr-111/delta Arg-113 as antagonist affinity determinants. *Biochemistry*. 1999;38(20):6689–98.
17. Chiara DC, Cohen JB. Identification of amino acids contributing to high and low affinity D-tubocurarine sites in the torpedo nicotinic acetylcholine receptor. *J Biol Chem*. 1997;272(52):32940–50.
18. Sine SM, Kreienkamp HJ, Bren N, Maeda R, Taylor P. Molecular dissection of subunit interfaces in the acetylcholine receptor: identification of determinants of alpha-conotoxin M1 selectivity. *Neuron*. 1995;15(1):205–11.
19. Bren N, Sine SM. Identification of residues in the adult nicotinic acetylcholine receptor that confer selectivity for curariform antagonists. *J Biol Chem*. 1997;272(49):30793–8.
20. Unwin N. Refined structure of the nicotinic acetylcholine receptor at 4Å resolution. *J Mol Biol*. 2005;346(4):967–89.
21. Bocquet N, Prado de Carvalho L, Cartaud J, Neyton J, Le Poupon C, Taly A, Grutter T, Changeux JP, Corringer PJ. A Prokaryotic proton-gated ion channel from the nicotinic acetylcholine receptor family. *Nature*. 2007;445(7123):116–9.
22. Bocquet N, Nury H, Baaden M, Le Poupon C, Changeux JP, Delarue M, Corringer PJ. X-ray structure of a pentameric ligand-gated ion channel in an apparently open conformation. *Nature*. 2009;457(7225):111–4.
23. Sauguet L, Poitevin F, Murail S, Van Renterghem C, Moraga-Cid G, Malherbe L, Thompson AW, Koehl P, Corringer PJ, Baaden M, Delarue M. Structural basis for ion permeation mechanism in pentameric ligand-gated ion channels. *EMBO J*. 2013;32(5):728–41.
24. Prevost MS, Sauguet L, Nury H, Van Renterghem C, Huon C, Poitevin F, Baaden M, Delarue M, Corringer PJ. A locally closed conformation of a bacterial pentameric proton-gated ion channel. *Nat Struct Mol Biol*. 2012;19(6):642–9.

25. Grosman C, Salamone FN, Sine SM, Auerbach A. The extracellular linker of muscle acetylcholine receptor channels is a gating control element. *J Gen Physiol.* 2000;116(3):327–40.
26. Kash TL, Jenkins A, Kelley JC, Trudell JR, Harrison NL. Coupling of agonist binding to channel gating in the GABA(A) receptor. *Nature.* 2003;421(6920):272–5.
27. Katz B, Thesleff S. A study of the 'Desensitization' produced by acetylcholine at the motor endplate. *J Physiol.* 1957;138:63–80.
28. Neubig RR, Boyd ND, Cohen JB. Conformations of Torpedo acetylcholine receptor associated with ion transport and desensitization. *Biochemistry.* 1982;21(14):3460–7.
29. Boyd ND, Cohen JB. Desensitization of membrane-bound Torpedo acetylcholine receptor by amine noncompetitive antagonists and aliphatic alcohols: studies of [3H]acetylcholine binding and 22Na⁺ ion fluxes. *Biochemistry.* 1984;23(18):4023–33.
30. Cohen JB, Correll LA, Dreyer EB, Kuisk IR, Medynski DC, Strnad NP. Interactions of local anesthetics with torpedo nicotinic acetylcholine receptors. In: Roth SH, Miller KW, editors. *Molecular and cellular mechanisms of anesthetics.* New York: Plenum Publishing Corporation; 1986. p. 111–24.
31. Oswald RE. Binding of phencyclidine to the detergent solubilized acetylcholine receptor from Torpedo marmorata. *Life Sci.* 1983;32(10):1143–9.
32. Oswald RE, Heidmann T, Changeux JP. Multiple affinity states for noncompetitive blockers revealed by [3H]phencyclidine binding to acetylcholine receptor rich membrane fragments from Torpedo marmorata. *Biochemistry.* 1983;22(13):3128–36.
33. Middleton RE, Strnad NP, Cohen JB. Photoaffinity labeling the torpedo nicotinic acetylcholine receptor with [(3H)]tetracaine, a nondesensitizing noncompetitive antagonist. *Mol Pharmacol.* 1999;56(2):290–9.
34. Herz JM, Atherton SJ. Steric factors limit access to the noncompetitive inhibitor site of the nicotinic acetylcholine receptor. Fluorescence studies. *Biophys J.* 1992;62(1):74–6.
35. Boyd ND, Cohen JB. Kinetics of binding of [3H]acetylcholine to Torpedo postsynaptic membranes: association and dissociation rate constants by rapid mixing and ultrafiltration. *Biochemistry.* 1980;19(23):5353–8.
36. Boyd ND, Cohen JB. Kinetics of binding of [3H]acetylcholine and [3H]carbamoylcholine to Torpedo postsynaptic membranes: slow conformational transitions of the cholinergic receptor. *Biochemistry.* 1980;19(23):5344–53.
37. Grosman C, Zhou M, Auerbach A. Mapping the conformational wave of acetylcholine receptor channel gating. *Nature.* 2000;403(6771):773–6.
38. Auerbach A. The gating isomerization of neuromuscular acetylcholine receptors. *J Physiol.* 2010;588(Pt 4):573–86.
39. Cymes GD, Grosman C, Auerbach A. Structure of the transition state of gating in the acetylcholine receptor channel pore: a phi-value analysis. *Biochemistry.* 2002;41(17):5548–55.
40. Koshland Jr DE, Nemethy G, Filmer D. Comparison of experimental binding data and theoretical models in proteins containing subunits. *Biochemistry.* 1966;5(1):365–85.
41. Xiu X, Puskar NL, Shanata JA, Lester HA, Dougherty A. Nicotine binding to brain receptors requires a strong cation- π interaction. *Nature.* 2009;458(7237):534–7.
42. Beene DL, Brandt GS, Zhong W, Zacharias NM, Lester HA, Dougherty DA. Cation- π interactions in ligand recognition by serotonergic (5-HT_{3A}) and nicotinic acetylcholine receptors: the anomalous binding properties of nicotine. *Biochemistry.* 2002;41(32):10262–9.
43. Auerbach A. The energy and work of a ligand-gated ion channel. *J Mol Biol.* 2013; 425(9):1461–75.
44. Labarca C, Nowak MW, Zhang H, Tang L, Deshpande P, Lester HA. Channel gating governed symmetrically by conserved leucine residues in the M2 domain of nicotinic receptors. *Nature.* 1995;376(6540):514–6.
45. Unwin N. Acetylcholine receptor channel imaged in the open state. *Nature.* 1995; 373(6509):37–43.
46. Unwin N. Nicotinic acetylcholine receptor at 9 Å resolution. *J Mol Biol.* 1993;229(4):1101–24.
47. Miyazawa A, Fujiyoshi Y, Unwin N. Structure and gating mechanism of the acetylcholine receptor pore. *Nature.* 2003;423(6943):949–55.

48. Pascual JM, Karlin A. State-dependent accessibility and electrostatic potential in the channel of the acetylcholine receptor. Inferences from rates of reaction of thiosulfonates with substituted cysteines in the M2 segment of the alpha subunit. *J Gen Physiol.* 1998;111(6):717–39.
49. Beckstein O, Sansom MS. A hydrophobic gate in an ion channel: the closed state of the nicotinic acetylcholine receptor. *Phys Biol.* 2006;3(2):147–59.
50. Cymes GD, Ni Y, Grosman C. Probing Ion-channel pores One proton at a time. *Nature.* 2005;438(7070):975–80.
51. Burzomato V, Beato M, Groot-Kormelink PJ, Colquhoun D, Sivilotti LG. Single-channel behavior of heteromeric alpha1beta glycine receptors: an attempt to detect a conformational change before the channel opens. *J Neurosci.* 2004;24(48):10924–40.
52. Lape R, Colquhoun D, Sivilotti LG. On the nature of partial agonism in the nicotinic receptor superfamily. *Nature.* 2008;454(7205):722–7.
53. Lape R, Krashia P, Colquhoun D, Sivilotti LG. Agonist and blocking actions of choline and tetramethylammonium on human muscle acetylcholine receptors. *J Physiol.* 2009;587(Pt 21):5045–72.
54. Purohit P, Auerbach A. Loop C and the mechanism of acetylcholine receptor-channel gating. *J Gen Physiol.* 2013;141(4):467–78.
55. Steinbach JH, Sine SM. Function of nicotinic acetylcholine receptors. *Soc Gen Physiol Ser.* 1987;41:19–42.
56. Papke RL. Enhanced inhibition of a mutant neuronal nicotinic acetylcholine receptor by agonists: protection of function by (E)-N-methyl-4-(3-pyridinyl)-3-butene-1-amine (TC-2403). *J Pharmacol Exp Ther.* 2002;301(2):765–73.
57. Papke RL, Thinschmidt JS. The correction of alpha7 nicotinic acetylcholine receptor concentration-response relationships in *Xenopus* oocytes. *Neurosci Lett.* 1998;256(3):163–6.
58. Jackson MB. Perfection of a synaptic receptor: kinetics and energetics of the acetylcholine receptor. *Proc Natl Acad Sci U S A.* 1989;86(7):2199–203.
59. Song XZ, Andreeva IE, Pedersen SE. Site-selective agonist binding to the nicotinic acetylcholine receptor from *Torpedo californica*. *Biochemistry.* 2003;42(14):4197–207.
60. White BH, Cohen JB. Agonist-induced changes in the structure of the acetylcholine receptor M2 regions revealed by photoincorporation of an uncharged nicotinic noncompetitive antagonist. *J Biol Chem.* 1992;267(22):15770–83.
61. White BH, Howard S, Cohen SG, Cohen JB. The hydrophobic photoreagent 3-(trifluoromethyl)-3-m-([125I] iodophenyl) diazirine is a novel noncompetitive antagonist of the nicotinic acetylcholine receptor. *J Biol Chem.* 1991;266(32):21595–607.
62. White BH, Cohen JB. Photolabeling of membrane-bound *Torpedo* nicotinic acetylcholine receptor with the hydrophobic probe 3-trifluoromethyl-3-(m-[125I]iodophenyl)diazirine. *Biochemistry.* 1988;27(24):8741–51.
63. Chiara DC, Hamouda AK, Ziebell MR, Mejia LA, Garcia 3rd G, Cohen JB. [(3)H]chlorpromazine photolabeling of the *torpedo* nicotinic acetylcholine receptor identifies two state-dependent binding sites in the ion channel. *Biochemistry.* 2009;48(42):10066–77.
64. Heidmann T, Changeux JP. Time-resolved photolabeling by the noncompetitive blocker chlorpromazine of the acetylcholine receptor in its transiently open and closed ion channel conformations. *Proc Natl Acad Sci U S A.* 1984;81(6):1897–901.
65. Oswald R, Changeux JP. Ultraviolet light-induced labeling by noncompetitive blockers of the acetylcholine receptor from *Torpedo marmorata*. *Proc Natl Acad Sci U S A.* 1981;78(6):3925–9.
66. Heidmann T, Oswald RE, Changeux JP. Multiple sites of action for noncompetitive blockers on acetylcholine receptor rich membrane fragments from *torpedo marmorata*. *Biochemistry.* 1983;22(13):3112–27.
67. Herz JM, Kolb SJ, Erlinger T, Schmid E. Channel permeant cations compete selectively with noncompetitive inhibitors of the nicotinic acetylcholine receptor. *J Biol Chem.* 1991;266(25):16691–8.
68. Herz JM, Johnson DA, Taylor P. Interaction of noncompetitive inhibitors with the acetylcholine receptor. The site specificity and spectroscopic properties of ethidium binding. *J Biol Chem.* 1987;262(15):7238–47.

69. Rankin SE, Addona GH, Kloczewiak MA, Bugge B, Miller KW. The cholesterol dependence of activation and fast desensitization of the nicotinic acetylcholine receptor. *Biophys J*. 1997;73(5):2446–55.
70. Lurtz MM, Hareland ML, Pedersen SE. Quinacrine and ethidium bromide bind the same locus on the nicotinic acetylcholine receptor from *Torpedo californica*. *Biochemistry*. 1997;36(8):2068–75.
71. Pratt MB, Pedersen SE, Cohen JB. Identification of the sites of incorporation of [3H]ethidium diazide within the *Torpedo* nicotinic acetylcholine receptor ion channel. *Biochemistry*. 2000;39(37):11452–62.
72. Sine SM, Steinbach JH. Activation of acetylcholine receptors on clonal mammalian BC3H-1 cells by high concentrations of agonist. *J Physiol*. 1987;385:325–59.
73. Elenes S, Auerbach A. Desensitization of diliganded mouse muscle nicotinic acetylcholine receptor channels. *J Physiol*. 2002;541(Pt 2):367–83.
74. Yamodo IH, Chiara DC, Cohen JB, Miller KW. Conformational changes in the nicotinic acetylcholine receptor during gating and desensitization. *Biochemistry*. 2010;49(1):156–65.
75. Arevalo E, Chiara DC, Forman SA, Cohen JB, Miller KW. Gating-enhanced accessibility of hydrophobic sites within the transmembrane region of the nicotinic acetylcholine receptor's {delta}-subunit. A time-resolved photolabeling study. *J Biol Chem*. 2005;280(14):13631–40.
76. Heidmann T, Bernhardt J, Neumann E, Changeux JP. Rapid kinetics of agonist binding and permeability response analyzed in parallel on acetylcholine receptor rich membranes from *Torpedo marmorata*. *Biochemistry*. 1983;22(23):5452–9.
77. Monod J, Wyman J, Changeux J-P. On the nature of allosteric transitions: a plausible model. *J Mol Biol*. 1965;12(1):88–118.
78. Purohit P, Bruhova I, Auerbach A. Sources of energy for gating by neurotransmitters in acetylcholine receptor channels. *Proc Natl Acad Sci U S A*. 2012;109(24):9384–9.
79. Rayes D, De Rosa MJ, Sine SM, Bouzat C. Number and locations of agonist binding sites required to activate homomeric Cys-loop receptors. *J Neurosci*. 2009;29(18):6022–32.
80. Campo-Soria C, Chang Y, Weiss DS. Mechanism of action of benzodiazepines on GABAA receptors. *Br J Pharmacol*. 2006;148(7):984–90.
81. Shen XM, Ohno K, Tsujino A, Brengman JM, Gingold M, Sine SM, Engel AG. Mutation causing severe myasthenia reveals functional asymmetry of AChR signature cystine loops in agonist binding and gating. *J Clin Invest*. 2003;111(4):497–505.
82. Humphrey W, Dalke A, Schulten K. VMD: visual molecular dynamics. *J Mol Graph*. 1996;14(1):33–8,27–8.

Nicotinic Receptors

Lester, R.A.J. (Ed.)

2014, XVII, 461 p. 42 illus., 31 illus. in color., Hardcover

ISBN: 978-1-4939-1166-0

A product of Humana Press